*Science of Sintering*, **39** (2007) 281-286

doi: 10.2298/SOS0703281R

UDK 677.026.34:553.689

# Raman Study Of Ba-Doped Ceria Nanopowders

**M. Radović[1*)], Z. Dohčević-Mitrović[1], M. Šćepanović[1], M. Grujić-Brojčin[1], B. Matović[2], S. Bošković[2] Z. V. Popović[1]**

[1]Institute of Physics, Center for Solid State Physics and New Materials, Pregrevica 118, P.O. Box 68, 11080 Belgrade, Serbia,

[2]Institute of Nuclear Sciences 'Vinca', 11001 Belgrade, Serbia

***Abstract:***

*A series of $Ce_{1-x}Ba_xO_{2-y}$ ($5 \le x \le 0.20$) nanometric powders were synthesized by self-propagating room temperature synthesis. XRD and Raman scattering measurements were used to characterize the samples at room temperature. All the samples are solid solutions with fluorite type structure with an average crystallite size about 5 nm. The redshift and asymmetric broadening of the Raman $F_{2g}$ mode can be well explained with combined confinement and strain effects because of the nanocrystalline powders nature. The appearance of the additional peaks at ~560 $cm^{-1}$ and ~600 $cm^{-1}$, are attributed to extrinsic and intrinsic $O^{2-}$ vacancies in ceria lattice. Raman spectra of temperature treated $Ce_{0.80}Ba_{0.20}O_{2-\delta}$ sample revealed the instability of this system.*

***Keywords:*** *Ba doped ceria nanopowders, XRD method, Raman scattering, phase separation*

## 1. Introduction

Cerium dioxide is of interest because of its multiple applications such as catalysis in vehicle emissions-control systems [1], high storage capacitors [2], for high Tc superconducting structures [3], and for optical devices [4]. Recently, ceria based solid solutions have gained an increasing amount of attention due to their potential use as electrolyte material in solid oxide fuel cells [5] (SOFCs). Optimization of SOFCs, to operate at reduced temperatures can be performed with use of electrolyte materials, which have high ionic conductivity at moderate temperatures.

Monodisperse cerium nanoparticles have higher ionic conductivities than bulk material, due to the properties related to their nanostructured nature. Nanosized ceria doped with oxides of di- or trivalent metals exhibits high ionic conductivity at intermediate temperatures (400-700 $^0$C) and is a promising candidate for electrolyte SOFCs materials. Whenever the $Ce^{4+}$ ions are replaced with di- or trivalent rare earth ions large density of oxygen vacancies are formed in ceria lattice enhancing the ionic conductivity of these materials [6,7]. The ionic conductivity significantly depends on the ionic radius and the concentration of the dopant too [8,9].

In the present work we described briefly the SPRT method as a possible method for preparing Ba-doped ceria nanopowders. To the best of our knowledge this method is for the first time used to synthesize the $Ce_{1-x}Ba_xO_{2-y}$ ($5 \le x \le 0.20$) solid solutions. The influence of

*) Corresponding author: marrad@phy.bg.ac.yu

doping and heating treatment on the Raman spectra of doped ceria powders is also investigated. Raman spectroscopy at room temperature was used to identify and distinguish the presence of oxygen vacancies introduced into ceria lattice with doping from the intrinsic vacancies that originate from nonstoichiometry in doped samples.

## 2. Experiment

The solid solutions of Ba doped $CeO_2$ samples were prepared by a self-propagating room temperature synthesis (SPRT) using metal nitrates and sodium hydroxide as the starting materials. The synthesis involves hand-mixing starting materials in alumina mortar for 5-7 minutes until the mixture got light brown. After being exposed to air for 3h, the mixture was suspended in water. Rinsing out of reaction byproduct ($NaNO_3$) was performed by centrifuge Centurion 1020D at 3500 rpm. This procedure was performed 3 times with distilled water and twice with ethanol [10].

Single solid-state solutions were obtained according to reaction:

$$2[(1-x)Ce(NO_3)_3 6H_2O + xBaNO_3] + 6NaOH + (1/y)O_2 \rightarrow 2Ce_{1-x}Ba_xO_{2-y} + 6NaNO_3 + 9H_2O$$

Compositions of $Ce_{1-x}Ba_xO_{2-y}$ were synthesized with x ranging from 0.05 to 0.20

The crystalline phases were identified by X-ray powder diffraction using Siemens D5000 diffractometer with Cu $K_\alpha$ radiation at room temperature. Diffractograms of the $Ce_{1-x}Ba_xO_{2-y}$ samples were recorded over the 2θ range from $20^0$ to $80^0$ using a position sensitive detector with $8^0$ acceptance angle. The average grain size was measured from the (111) XRD peak using the Scherrer formula. The average crystallite size was estimated to be 5 nm.

Room temperature Raman measurements were performed in the backscattering geometry using 514.5-nm line of Ar-ion laser, Jobin-Yvon U1000 monochromator and photomultiplier as a detector while high temperature Raman measurements were taken with same $Ar^+$ laser line using Jobin Yvon T64000 spectrometer equipped with Linkam TS 1500 microscope heating stage and nitrogen cooled charge-coupled-device detector (CCD). Overheating of the samples was avoided using a minimal laser power when no changes of the Raman spectra were noticed.

## 3. Results and discussion

According to the XRD spectra, Ba doped samples appeared to be of single phase for the whole doping range retaining the $CeO_2$ fluorite structure. Diffraction lines of Ba oxide were not registered in the whole doping range.

The XRD patterns for $Ce_{0.95}Ba_{0.05}O_{2-y}$, $Ce_{0.90}Ba_{0.10}O_{2-y}$ and $Ce_{0.85}Ba_{0.15}O_{2-y}$ samples are shown in Fig. 1 (a). Change of lattice parameter as a function of dopant concentration is shown in Fig.1 (b). Lattice parameter of pure $CeO_2$ is shown as reference one. The increasing of lattice constant with increasing dopant concentration is directly correlated with ionic size $CeO_2$ with a fluorite structure has one Raman active triply degenerate $F_{2g}$ mode at 465 $cm^{-1}$.

This mode presents symmetrical stretching vibrations of $CeO_8$ vibrational unit and should be very sensitive to the oxygen sublattice disorder [11]. Raman study of $CeO_2$ nanoparticles have demonstrated that the $F_{2g}$ mode shifts to lower energies with increasing linewidth while the line shape becomes asymmetric on the low-energy side as the particle size gets smaller [12]. This evolution of the Raman line can be attributed to the combined effect of phonon confinement and inhomogeneous strain [12,13]. To explain properly the evident phonon softening and increased linewidth asymmetry of the main $F_{2g}$ mode in the $Ce_{1-x}Ba_xO_{2-y}$ samples we used the phonon confinement model (PCM) that incorporates size and strain effects [13]. Raman intensity is calculated over the whole Brillouin zone by the following relation:

$$I(\omega) = \sum_{1}^{3} \int_{0}^{\infty} \rho(L)dL \int_{BZ} \frac{\exp(-\frac{q^2 L^2}{8\beta})}{[\omega - (\omega_i(q) + \Delta\omega_i(q,L))]^2 + [\Gamma_0 / 2]^2} d^3 q \quad (1)$$

where ρ(L) is Gaussian particle size distribution, L is particle size and $\Gamma_0$ is the linewidth of the Raman mode in bulk crystal. The factor β is an adjustable parameter depending on the strength of the phonon confinement in different nanomaterials. It varies from β=1 to $\beta=2\pi^2$ for Richter [14] and Cambpell [15] model respectively. In order to obtain the best fits of our experimental spectra we used higher degree of phonon confinement $\beta\sim4\pi^2$.

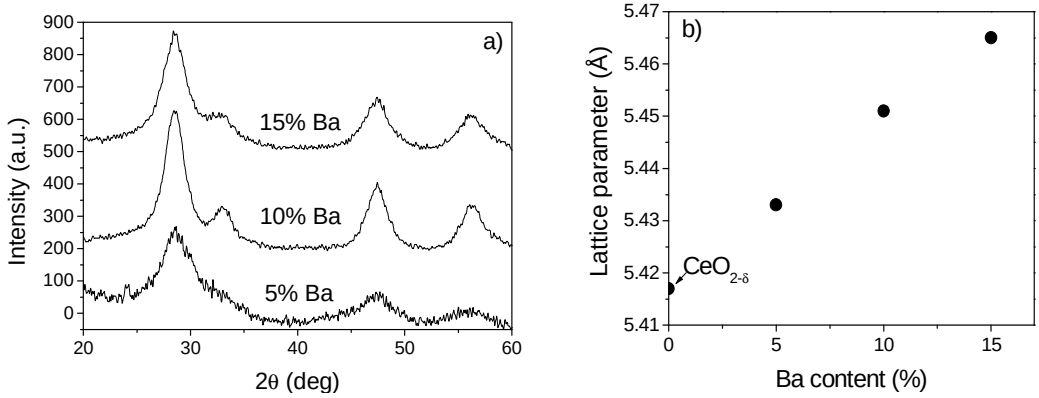


**Fig. 1** a) XRD spectra of $Ce_{0.95}Ba_{0.05}O_{2-y}$, $Ce_{0.90}Ba_{0.10}O_{2-y}$ and $Ce_{0.85}Ba_{0.15}O_{2-y}$ samples b) change of lattice parameter with dopant concentration.

Fig. 2 shows Raman spectra at room temperature of the Ba doped $CeO_2$ samples (circles) and numerical fits of the experimental data (lines) using PCM (Eq. 1).

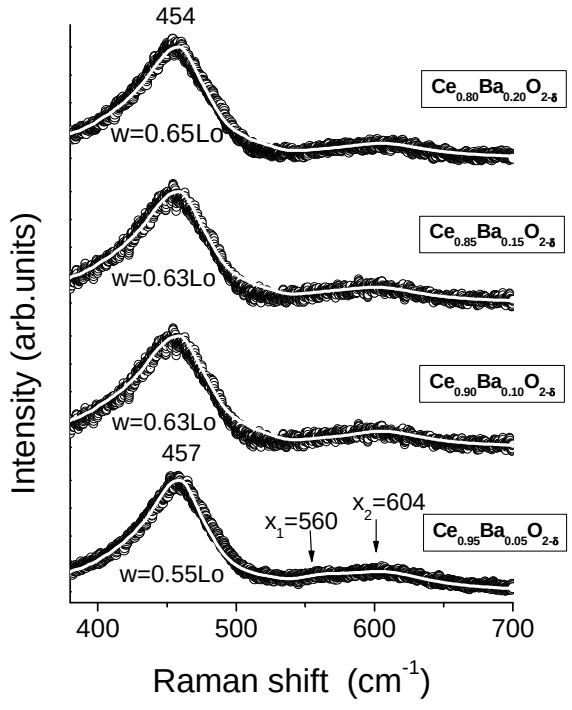


**Fig. 2** Raman spectra of Ba doped $CeO_2$ samples at room temperature.

The best accordance between the experimental and calculated curves is obtained for the average particle size $L$=6.6 nm value while the Gaussian width ($w$) is also given in Fig. 2 for each sample. As can be seen Raman spectra of $Ce_{1-x}Ba_xO_{2-y}$ samples show systematic shift of the $F_{2g}$ mode, positioned at ~ 457 $cm^{-1}$ for the lowest Ba doping concentration, to lower frequencies with increasing doping level (in a $Ce_{0.80}Ba_{0.20}O_{2-\delta}$ this mode is positioned at ~ 454 $cm^{-1}$) while the linewidth increases. Such a decrease in phonon energy is consistent with dilatation of unit cell parameter due to the incorporation of large $Ba^{2+}$ ions in cerium lattice. On the other hand the broadening of the $F_{2g}$ mode with increasing Ba content could be correlated with increasing $O^{2-}$ vacancy concentration with doping because this mode is very sensitive to disorder in oxygen sub-lattice [11].

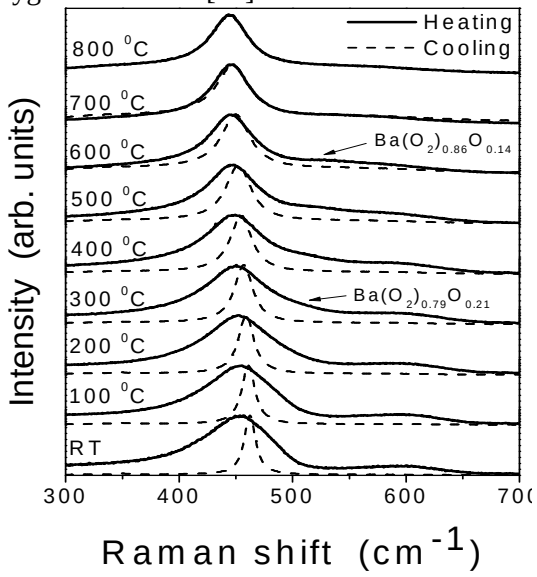


**Fig. 3** Raman spectra of $Ce_{0.85}Ba_{0.20}O_{2-y}$ sample during heating and cooling.

Besides the $F_{2g}$ Raman mode there are two additional modes at ~ 560 $cm^{-1}$ and ~ 600 $cm^{-1}$. These modes are assigned to the extrinsic oxygen vacancies introduced into the ceria lattice by substitution of $Ce^{4+}$ ions with $Ba^{2+}$ ions and intrinsic oxygen vacancies due to the nonstoichiometry of ceria nanopowders [5, 10].

One sample with the highest Ba concentration ($Ce_{0.80}Ba_{0.20}O_{2-\delta}$) was temperature treated in order to investigate the phonon behaviour and stability of this system at high temperatures. Raman spectra of $Ce_{0.80}Ba_{0.20}O_{2-\delta}$ sample, obtained by heating (lines) and gradual cooling (dashed lines) are shown in Fig. 3. Temperature dependence of mode frequency upon heating and cooling is shown in Fig. 4.

We have found that frequency and linewidth of the $F_{2g}$ mode continuously decreases by heating while the line shape becomes more symmetric up to 800 $^0$C when it becomes totally symmetric. In the Raman spectra at 300 $^0$C additional mode can be observed at 515 $cm^{-1}$. This mode can be ascribed to the Raman mode of $Ba(O_2)_{0.79}O_{0.21}$ system [16]. Frequency of this mode increases with temperature increase up to 527 $cm^{-1}$ at 600$^o$C, which corresponds to the frequency of the $Ba(O_2)_{0.86}O_{0.14}$ system [16]. This mode disappears as the temperature further increases to 700$^o$C. Therefore we concluded that at 300$^o$C phase separation begins and certain types of $Ba(O_2)_{1-x}O_x$ oxide system are formed. At higher temperatures these oxides are unstable. This conclusion is valid if we have in mind that barium oxide (peroxide) begins to decompose at 500$^o$C in air [17].

Two competitive effects could be responsible for frequency and linewidth change during heating: anharmonic and size effects. If the anharmonic effects are dominant we would expect the frequency red shift and linewidth increase with temperature, while the expected

particle growth with temperature would produce an opposite trend. The frequency shift is consistent with the theory regarding the anharmonic effects in crystals [18] but the linewidth behaviour is not. The only plausible explanation for that is that phase separation on $CeO_2$ and $Ba(O_2)_{1-x}O_x$ takes place in $Ce_{1-x}Ba_xO_{2-\delta}$ samples during heating and at temperatures higher than 600 $^0$C Ba disappears from the ceria lattice. By cooling the frequency increases, reaching the value of 462.5 cm$^{-1}$ at room temperature. Linewidth continuously decreases, during cooling, down to 12.3 cm$^{-1}$ at room temperature. This behavior is typical for the anharmonic phonon behaviour in bulk samples and similar to that found in a $CeO_2$ polycrystalline sample [12] leading us to conclude that the $Ce_{0.80}Ba_{0.20}O_{2-\delta}$ sample transforms from nano to a polycrystalline $CeO_2$ sample by the above mentioned temperature treatment.

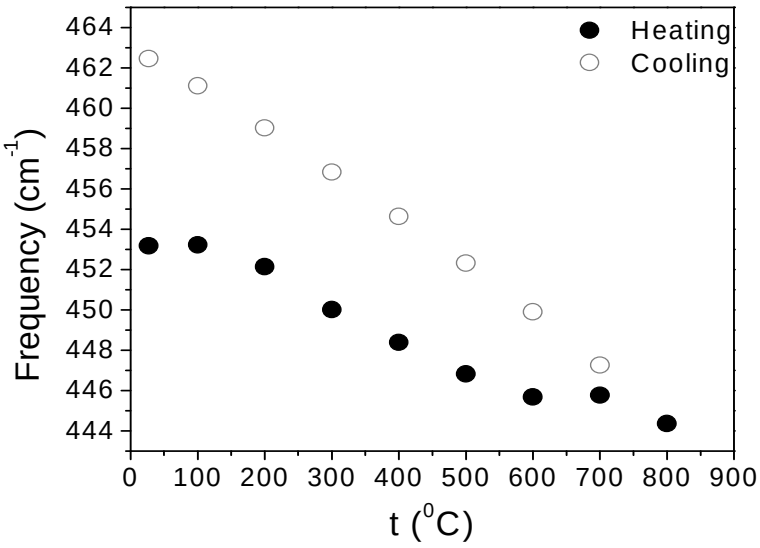


**Fig. 4** Temperature dependence of $F_{2g}$ mode frequency

Intensity of modes at 560 cm$^{-1}$ and 600 cm$^{-1}$ increases with temperature increase until 300 $^0$C when they start to decrease in intensity and become very weak at 800 $^0$C. This means that the concentration of oxygen vacancies decreases with temperature. The sample becomes more stoichiometric and the structure defects are probably removed by heat treatment.

## 4. Conclusions

In summary, $Ce_{1-x}Ba_xO_{2-\delta}$ nanocrystalline samples ($5 \leq x \leq 0.20$) were prepared by the SPRT method. From XRD and Raman measurements at room temperature we have concluded that $Ce_{1-x}Ba_xO_{2-\delta}$ samples are solid solutions with fluorite crystal structure in the whole doping range. The Raman spectra are well described using a spatial correlation model with combined size and inhomogeneous strain effects. At high temperatures a phase separation takes place between $CeO_2$ and $Ba(O_2)_{1-x}O_x$ systems. We demonstrated that Raman spectroscopy is a very effective diagnostic method in monitoring nanocrystalline size, detecting phase separation and the presence of intrinsic and introduced oxygen vacancies in the ceria lattice.

## Acknowledgements

This work was supported by the MSRS under the project No. 141047 and the OPSA-026283 Project within the EC FP6 Programme and SASA Project F/134.

## References

1. A. Trovarelli, Catal. Rev. Sci. Eng. 38 (1996) 439.
2. Z. Zhang, X. Du, W. Wang, J. Vac. Sci. Tech. A 18 (2000) 2928.
3. A. Walkenhorst, M. Schmitt, H. Adrian, K. Petersen, Appl. Phys. Lett. 64 (1994) 1871.
4. S. Kanakaraju, S. Mohan, A. K. Sood, Thin Solid Films 305 (1997) 191.
5. Z. Dohcevic-Mitrovic, M. Grujic-Brojcin, M. Scepanovic, Z. V. Popovic, S. Boskovic, B. Matovic, M. Zinkevich, F. Aldinger, J. Phys. Cond. Matt. 18 (2006) 1.
6. A. Sin, Y. Dubitsky, A, Zaopo, S. A. Aric`o, L. Gullo, D. La Rosa, S. Siracusano, V. Antonucci, C. Oliva, O. Ballabio, Solid State Ion. 175 (2004) 361.
7. C. Peng, Y. Wang, K. Jiang, Q. B. Bin, W. H. Liang, J. Feng and J. Meng, J. Alloys Compounds 349 **(**2003) 273.
8. H. Deguchi, H. Yoshida, T. Inagaki, M. Horiuchi, Solid State Ionics 176 (2005) 1817.
9. L. Minervini, M. O. Zacate, R. W. Grimes, Solid State Ionics 116 (1997) 339.
10. S. Boskovic, D. Djurovic, B. Matovic, M. Cancarevic, Z. Mitrovic-Dohcevic, Z. V. Popovic, M. Zinkevich, F. Aldinger, Materials Science Forum, 518 (2006) 95.
11. I. Kosacki, T. Suzuki, H. Anderson, P. Colomban, Solid State Ionics 149 (2002) 99.
12. J. E. Spanier, R. D. Robinson, F. Zhang, S. W. Chan, I. P. Herman, Phys. Rev. B 64 (2001) 245407.
13. Z. Dohcevic-Mitrovic, M. Grujic-Brojcin, M. Scepanovic, Z. V. Popovic, S. Boskovic, B. Matovic, M. Zinkevich, F. Aldinger, Solid State Commun. 137 (2006) 387.
14. H. Richter, Z. Wang, L. Ley, Solid State Commun. 39 (1981) 625.
15. I. H. Campbell, P. M. Fauchet, Solid State Commun. 58 (1986) 739.
16. D. de Waal, K. Range, M. Konigstein, W. Kiefer, J. Raman Spect. 29 (1998)109.
17. J. H. Lunsford, X. Yang, K. Haller, J. Laane, J. Phys. Chem. 97 (1993) 13810.
18. M. Balkanski, R.F. Wallis, E. Haro, Phys. Rev. B 28 (1983) 1928.

***Садржај:*** *Серија нанопрахова $Ce_{1-x}Ba_xO_{2-y}$ $(5 \leq x \leq 0.20)$, добијена је методом самораспростирује синтезе на собној температури (SPRT). За карактеризацију узорака коришћене су методе дифракције рендгенских зрака (XRD)и Раман спектроскопије.Сви узорци су чврсти раствори флуоритне структуре чија је средња величина кристалиа око 5nm. Померај Раман $F_{2g}$ мода ка нижим енергијама и његово асиметрично ширење може се објаснити комбинованим ефектима фононског конфајнмента и стрејна. Појава додатних модова на ~560 $cm^{-1}$ и ~600 $cm^{-1}$, приписује се постојању уведених и својствених $O^{2-}$ вакансија у церијумовој решетки. Раман спектри одгреваног $Ce_{0.80}Ba_{0.20}O_{2-\delta}$ узорка указују на нестабилност овог система.*

***Кључне речи:*** *Ba допирани нанопрахови церијума, XRD метод, Рамановo расејање, сепарација фаза.*